

On the potential for regolith control of fluvial terrace formation in semi-arid escarpments

Kevin P. Norton¹, Fritz Schlunegger², Camille Litty²

[1]{School of Geography, Environment and Earth Sciences, Victoria University of Wellington, New Zealand}

[2]{Institute of Geological Sciences, University of Bern, Switzerland}

Correspondence to: K.P. Norton (kevin.norton@vuw.ac.nz)

Abstract

Cut-fill terraces occur throughout the western Andes where they have been associated with pluvial episodes on the Altiplano. The mechanism relating increased rainfall to sedimentation is however not well understood. Here, we apply a hillslope sediment model and reported cosmogenic nuclide concentrations in terraces to examine terrace formation in semi-arid escarpment environments. We focus on the Rio Pisco system in western Peru in order to determine probable hillslope processes and sediment transport conditions during phases of terrace formation. Specifically, we model steady state and transient hillslope responses to increased precipitation rates. The measured terrace distribution and reconstructed sediment loads measured for the Rio Pisco agree with the transient model predictions, suggesting strong climatic control on the cut-fill sequences in western Peru primarily through large variations in sediment load. Our model suggests that the ultimate control for these terraces is the availability of sediment on the hillslopes with hillslope stripping supplying large sediment loads early in wet periods. At the Rio Pisco, this is manifest as an approximately 4x increase in erosion rates during pluvial periods. We suggest that this mechanism may also control terrace occurrence in other semi-arid escarpment settings.

1 Introduction

High elevation plateaus are commonly associated with either passive margins (e.g. Africa, Sri Lanka, Australia) or large convergent mountain systems (e.g. Himalaya, Andes). In either case, erosion on the plateau edge leads to the formation of rapidly eroding escarpments adjacent to the more slowly eroding plateaus [e.g. *Seidl et al.*, 1996; *Weissel and Seidl*, 1997; *Matmon et al.*, 2002; *van der Beek et al.*, 2002; *von Blanckenburg et al.*, 2004; *Kober et al.*, 2006; *Vanacker et al.*, 2007]. In this paper, we suggest that weathering is a dominant control on escarpment rivers as it is responsible for the production of sediment through the formation of regolith. The antiquity of most of these plateaus suggests that they erode through parallel retreat [e.g. *Schlunegger et al.*, 2006] with somewhat constant topographic profiles. These large topographic gradients often result in orographic precipitation on the escarpment [e.g. *Bookhagen and Strecker*, 2008]. Since weathering is at least partially dependent on water supply (e.g. *White and Blum*, 1995a), regolith formation is also likely to be enhanced on the plateau, especially during wet phases.

Quaternary climate change has led to fluctuations in the available precipitation on both the plateaus and adjacent valleys. The fluvial cut and fill terrace systems, which are common in these settings, are typically attributed to this climate variability [*Bookhagen et al.*, 2006; *Steffen et al.*, 2009]. Using a climate-dependent regolith production algorithm (*Norton et al.*, 2014) coupled with simple sediment transport laws (e.g. *Tucker and Slingerland*, 1997), we investigate the effects of climate change in the form of precipitation variation on the hillslope system and propose that hillslope regolith production and stripping may control cut and fill sequences during the Late Quaternary.

2 Setting

We focus on the Rio Pisco drainage basin, situated on the western Andean margin at c. 17° S, central Peru. This stream flows from its headwaters at ~4000 m asl across the Altiplano Plateau before plunging into a deeply incised canyon. This region marks a broad knickzone, which connects the mostly non-incised Miocene Altiplano Plateau to the flat, low-lying coastal plains (Figure 1). The high elevation plateau is characterized by high precipitation rates and low erosion rates, while the knickzone exhibits lower precipitation rates but much faster erosion (Figure 2). The knickzone is interpreted to maintain its slope while eroding headward due to low erosion rates at the plateau margin (*Abbühl et al.*, 2011). Above the

Formatted: English (New Zealand)

Formatted: English (New Zealand)

Formatted: English (New Zealand)

Formatted: English (New Zealand)

Formatted: English (New Zealand)

Formatted: English (New Zealand)

Formatted: English (New Zealand)

Formatted: English (New Zealand)

1 knickzones, the streams are still graded to the Miocene baselevel. This high elevation plateau
2 could be the result of dynamic reorganization of river channels (Willett *et al.*, 2014) and/or the
3 uplift of the western Andes (e.g. Schlunegger *et al.*, 2006, Schildgen *et al.*, 2007). ~~The Along~~
4 ~~the knickzone, the~~ Rio Pisco is currently ~~at~~-under ~~sediment capacity~~ ~~capacity over the length~~
5 ~~of the knickzone~~ as evidenced by the narrow modern channel where the stream cuts into
6 valley fill and bedrock. The upper river reaches are primarily bedrock channels, while lower
7 reaches are alluvial. Downstream of the knickzone, the floodplain widens and the river
8 becomes braided, attesting to an excess of sediment.

9 A series of cut-fill terraces and debris flow deposits fill the widening channel to within ~40km
10 from the coast (e.g. Steffen *et al.*, 2009; Bekaddour *et al.*, 2014). These valley fills consist of
11 both fluvial conglomerates and hillslope-derived debris flow breccias, which could indicate
12 phases of landsliding (e.g. McPhillips *et al.*, 2014). We proceeded according to Litty *et al.*
13 (2015) and measured the exposed thickness and extent of >100 terraces in the Pisco Valley
14 (Figure 3). These were classified as fluvial (composed of moderately-well sorted, well-
15 rounded clast-supported cobbles) or colluvial (composed of poorly sorted, angular to sub-
16 rounded, matrix-supported clasts) (Figure 4). The terraces were correlated based on elevation
17 and composition.

18 ~~Steffen et al. [2009]~~ dated the Late Quaternary terraces, which are abundant in the lower
19 reaches downstream of the knickzone, from ~40 to 120 km downstream distance. The ages of
20 the terrace accumulation correspond with well-known wet periods in the western Andes (e.g.
21 Minchin, 47.8-36 ka and Tauca, 26-14.9 ka, Baker *et al.*, 2001a, 2001b; Fritz *et al.*, 2004;
22 Placzek *et al.*, 2006). As documented by Steffen *et al.* [2009], regolith is shed over ca. 10-15
23 ky timescales from the hillslopes as debris flows during these pluvial periods. These authors
24 suggested that increased rainfall resulted in increased erosion and thereby increased sediment
25 supply to the river, causing a phase of deposition in the valley, starting generally with debris
26 flows from the hillslopes. They argued that as hillslopes became depleted of sediment, the
27 river begins to incise again while discharge remains high. While this scenario is logical, it has
28 not been tested from a sediment transport oriented point of view. In this contribution, we
29 present a model linking the production of sediment through weathering with a sediment
30 transport model to explore the conditions leading to the formation of the Rio Pisco terraces.

Formatted: English (New Zealand)

Formatted: English (New Zealand)

Formatted: English (New Zealand)

Formatted: English (New Zealand)

Field Code Changed

1 3 Hillslope Regolith

2 The mechanisms and rates of weathered regolith production are commonly expressed in the
3 context of erosion rates such that slower erosion rates are associated with thicker soil cover.
4 The Western Andean margin of Peru provides a setting in which weathered regolith is thick
5 on the slowly eroding plateau, but nearly absent at low elevations despite even lower erosion
6 rates. This seeming contradiction is best explained by gradients in the governing climatic
7 variables. *White and Blum* [1995b] showed that solute fluxes from a global compilation of
8 granitic watersheds approach 0 as precipitation approaches 0. In order to best model this
9 gradient in soil thickness, we apply the climate dependent regolith production model of
10 *Norton et al* (2014), which was based on the temperature and precipitation dependent
11 weathering data of *White and Blum* [1995b]. The model predicts time-transgressive or steady
12 state soil production rates and soil thicknesses for a given mean annual temperature and mean
13 annual precipitation, and mean erosion rate. Temperature (T), precipitation (P), and silicate
14 mineral activation energy (E_a) set the maximum soil production rate (SPR_{max});

15
$$SPR_{max} = a_0 P e^{\frac{-E_a}{R} \left(\frac{1}{T} - \frac{1}{T_0} \right)}$$

16 where R is the gas constant, T_0 is 5°C , and $a_0 = 0.42$ is a precipitation scaling factor tuned to the Pisco
17 soil dataset (Norton et al., 2014). The instantaneous soil production rate (SPR) and change in soil
18 thickness are calculated as a function of soil depth (H);

19
$$SPR = SPR_{max} e^{-\alpha H}$$

20 and local mass balance;

21
$$\frac{dH}{dt} = a_0 P e^{\frac{-E_a}{R} \left(\frac{1}{T} - \frac{1}{T_0} \right)} e^{-\alpha H} - D$$

22 where $\alpha = 0.03 \text{ cm}^{-1}$ is the soil depth scalar (e.g. Heimsath et al., 1997) and D is the denudation rate,
23 Rapid soil production rates and thick soils are predicted for high temperatures and
24 precipitation amounts. Erosion rates are the ultimate control on the output soil thickness and
25 system response time.

26 3.1 Regolith thickness in the Rio Pisco drainage basin

27 We test the sensitivity of the *Norton et al.* (2014) model to the different input variables by
28 allowing one variable to change while holding the other two at the plateau value (Figure 5).

Formatted: Font: Italic, English (New Zealand)
Formatted: English (New Zealand)
Formatted: Font: Italic, English (New Zealand)
Formatted: English (New Zealand)
Formatted: Font: Italic, English (New Zealand)
Formatted: English (New Zealand), Subscript
Formatted: English (New Zealand)
Formatted: Font: Italic, English (New Zealand)
Formatted: English (New Zealand), Subscript
Formatted: English (New Zealand)
Formatted: English (New Zealand)
Formatted: English (New Zealand)
Formatted: Font: 12 pt, Italic, English (New Zealand)
Formatted: English (New Zealand)
Formatted: Font: 12 pt, Italic, English (New Zealand)
Formatted: English (New Zealand), Subscript
Formatted: English (New Zealand)
Formatted: English (New Zealand), Subscript
Formatted: English (New Zealand)
Formatted: English (New Zealand)
Formatted: English (New Zealand)
Formatted: English (New Zealand)
Formatted: English (New Zealand)
Formatted: English (New Zealand)
Formatted: Font: 12 pt, Italic, English (New Zealand)
Formatted: English (New Zealand)
Formatted: Superscript
Formatted: English (New Zealand)
Formatted: English (New Zealand)
Formatted: English (New Zealand)
Formatted: English (New Zealand)
Formatted: English (New Zealand)
Formatted: English (New Zealand)

1 Precipitation and erosion have the largest individual control on the calculated steady-state
2 regolith thickness. The temperature effect is, ~~however,~~ much smaller. As such, variations in
3 temperature (both intra- and inter-annual) are negligible compared to other parameters. If
4 regolith thicknesses were dependent on temperature alone, our model predicts a more or less
5 uniform blanket over the entire catchment, increasing slightly towards the coast as
6 temperatures get warmer. In contrast, regolith depth would decrease rapidly towards the coast
7 in a solely precipitation-dependent state, approaching 0 at ~100 km from the headwaters.
8 Finally, if erosion were the sole process controlling and limiting regolith thicknesses, the
9 value of this variable would be expected to decrease in the rapidly eroding knickzone, but to
10 thicken again farther downstream. We note that in all cases, a positive dependence of the
11 maximum soil production rate $\Phi_{\theta} \rightarrow SPR_{max}$ on erosion, as proposed by *Heimsath et al.* (2012),
12 would result in thicker soil cover over a wider range of erosion rates, but should not change
13 the overall distribution of soils from the model. The modeled regolith depths generally match
14 the sparse measured depths from ridgetops in the Pisco Valley (e.g. *Norton et al.*, 2014).
15 Ridgetops were sampled for soil depth as the hillslopes throughout the escarpment tend to be
16 stripped bare of weathered material in the modern climate. Additionally, the rugged terrain,
17 poor access and lack of drillings precluded the collection of further data.

Formatted: English (New Zealand)

Formatted: English (New Zealand)

Formatted: Font: Italic

Formatted: Subscript

Formatted: English (New Zealand)

19 3.2 Hillslope sediment delivery mechanisms

20 Sediment supply to the river was calculated by combining the climate dependent soil
21 production model (*Norton et al.*, 2014) with cosmogenic nuclide-derived denudation rates
22 (*Abbühl et al.*, 2010, 2011; *Bekaddour et al.*, 2014). To determine modern sediment supply,
23 we allow the Pisco river to erode at its long-term rate as determined by cosmogenic nuclides,
24 assuming no hillslope storage (an assumption vital to the cosmogenic nuclide methods as
25 well; e.g. *von Blanckenburg*, 2006). The modern discharge is taken as the basin integrated
26 precipitation rate, which decreases down river which yields an average discharge of 20 m³/s
27 along the coastal section. As such, we ignore the effects of evapotranspiration and infiltration,
28 but still capture a more realistic discharge for the Pisco, which is c. 23 m³/s as measuring at
29 the gauging station of Letrayoc (*Bekaddour et al.*, 2014).

30 We model two potential responses to increased rainfall during pluvial periods: steady state
31 increase in denudation rate, and transient stripping of hillslope sediment (Figure 6). Based on

1 cosmogenic nuclide concentrations from the Piura River in northwestern Peru, *Abbühl et al.*
2 (2010) showed that, at steady state, denudation rates increase exponentially with increasing
3 precipitation rates below the plateau edge but are independent of precipitation on the plateau.
4 Our first model assumes this relationship to hold in time as well as space. We therefore hold
5 the denudation rate constant on the plateau throughout time, but vary the denudation rate
6 below the plateau edge as $D_2 = D_1 * \exp^{cP}$ (where D_2 and D_1 are the predicted and initial
7 denudation rate (mm/yr), respectively, P is the mean annual precipitation (mm) and $c =$
8 0.0041 is empirically derived for the Western Andes; *Abbühl et al.*, 2010) up to the limit of
9 soil thickness (i.e. the maximum allowable erosion rate is the soil production rate). This
10 steady state model predicts a small but continuous increase in sediment load over the duration
11 of the pluvial period (e.g. Figure 6, 7a). Precipitation variability is modelled from the historic
12 averages from 1960 – 2003 for the rainfall stations in the immediate vicinity (Figures 1 and 7;
13 Agteca, 2010). The largest inter-annual variability occurs on the plateau where annual rainfall
14 is the highest. Relative rates are, however, highest near the coast where large single events
15 can more than double the annual averages (Figure 7b).

Formatted: English (New Zealand)

Formatted: English (New Zealand)

Formatted: English (New Zealand)

16 The transient model is based on the widespread presence of debris flow deposits in the
17 terraces and the rapid accumulation rates suggested by OSL dating (*Steffen et al.*, 2009).
18 These observations suggest that sediment is rapidly eroded from the hillslopes during pluvial
19 periods, resulting in a sediment pulse into the basin. To model this transient sediment
20 delivery, we assume complete hillslope stripping downstream of the knickzone (where slopes
21 are steep) upon initiation of the pluvial period followed by negligible erosion after the
22 hillslopes become bare of sediment (e.g. Figure 6 7b). We compare the longitudinal sediment
23 transport capacity/sediment load ratios to the existing terrace distribution in the Pisco valley.

25 4 Fluvial transport

26 The eroded material delivered to the channels will either be deposited or transported,
27 depending on the transport capacity of the stream. Channel flow and potential incision in
28 these streams are typically expressed in terms of shear stress and sediment transport
29 equations, and flow is driven by temporally variable (but spatially invariable) precipitation.

30 We begin by coupling the weathering-dependent model with an algorithm that describes
31 sediment transport in channels and apply it to the long profile of the Rio Pisco. Sediment

1 transport capacity T_c is calculated using the Bagnold equation [e.g. *Tucker and Slingerland*,
2 1994; 1997]:

$$3 T_c = \frac{BW}{(\rho_s - \rho_w)\rho^{1/2}g}(\tau - \tau_c)(\tau^{1/2} - \tau_c^{1/2}) \quad (1)$$

4
5
6 where B is a constant equal to 10 (e.g. *Hancock and Anderson*, 2002), W is channel width, ρ_s
7 and ρ_w are the densities of sediment and water, respectively, g is gravity, τ is the applied bed
8 shear stress, and τ_c is the critical shear stress for the entrainment of the D_{50} , which is the 50th
9 percentile grain size. Note that here we calculate sediment transport capacity, and the actual
10 sediment discharge is dependent on the sediment yield of the basin. We scale channel width to
11 discharge using the empirical downstream hydraulic geometry relationship [e.g. *Yalin*, 1992]
12 fit to the Rio Pisco:

$$13 W = aQ_w^b \quad (2)$$

14
15
16 where a is a constant and b is usually assumed to be 0.5 [e.g. *Tucker and Slingerland*, 1997].

17 Shear stress is calculated as:

$$18 \tau = \rho_w g \left(\frac{Q_w}{W} \right)^{3/5} n^{3/5} S^{7/10} \quad (3)$$

19
20
21 (after *Hancock and Anderson*, 2002) where Q_w is the water discharge, n is Manning's n , and S
22 is the channel gradient. Critical shear stress is calculated as

$$23 \tau_c = 0.047(\rho_s - \rho_w)gD_{50} \quad (4)$$

1 (e.g. Leopold et al., 1964) where D_{50} is the 50th percentile grain size, here taken to be the
2 mean grain size measured in the Pisco Valley terraces, 0.02 m (Litty et al., 2015). We applied
3 a Shield's parameter of 0.047, which is consistent with the suggestions proposed by Meyer-
4 Müller (1948) and Heller and Paola (1992) for these streams.

5 The cumulative sediment supply is calculated as the sum of the upstream hillslope erosional
6 fluxes contributing to point n along the channel:

$$7 \quad Q_s = \sum_{i=1}^n D_i A_i \quad (5)$$

Formatted: English (New Zealand)

Formatted: English (New Zealand)

9 and water discharge is likewise calculated as the sum of the upstream area and precipitation
10 amount,

$$11 \quad Q_w = \sum_{i=1}^n c P_i A_i \quad (6)$$

Formatted: English (New Zealand)

Formatted: English (New Zealand)

13
14 where A_i is the lateral contributing hillslope area (m^2) to point i in the channel, P_i is
15 precipitation (mm/yr) and D_i is erosion (mm/ky) from this area, and c is a runoff coefficient.
16 The runoff coefficient accounts for losses due to evapotranspiration and infiltration. Because
17 of a lack of data we assume in this study that $c=I$, however, it is likely that the coefficient is
18 smaller as evapotranspiration (e.g., Bloschl et al., 2013) and infiltration in the lower reaches
19 of the Rio Pisco lead to lower discharge downstream. In this case, T_c will decrease more
20 rapidly downstream.

21 The fluvial transport model, while simple in its approach, provides a first order estimate of
22 river response in this system. The 1D model is not capable of representing changes in fluvial
23 transport style or changing hydraulic parameters. This is especially noticeable in our
24 treatment of hydraulic geometry and shear stress which are calculated using empirical
25 relationships (e.g. Hancock and Anderson, 2002; Shields, 1936). We adopted this approach as
26 a more formal treatment of roughness and skin friction (e.g. Ferguson, 2007) would require
27 knowledge of flow velocity or depth which are lacking for the Rio Pisco. Despite these
28 limitations, the shear stress approach has been shown to adequately model strath terrace

1 formation which involves both erosion and deposition in the fluvial system (Hancock and
2 Anderson, 2002).

Formatted: English (New Zealand)

3 **4.1 Coupled hillslope-river model**

4 We apply the 1D coupled sediment transport - weathering dependent soil model to the Rio
5 Pisco using 1 km node spacing (Figure 7). All dependent variables are free to change at each
6 node (e.g. spatially variable denudation rates, precipitation rate, and temperature). We take
7 precipitation rates from the Global Historical Climatology Network compilation of *Agteca*
8 [2010], which are based on 493 individual rain gauges measured over 10 to 85 years (mean 20
9 years) within Peru. Temperature is determined for each node assuming an atmospheric lapse
10 rate of 6° C/km, and the mean annual temperature of 12.8° C of Cusco, Peru at 3204m
11 elevation a.s.l. For the Rio Pisco model inputs (Figure 2), we use the long-profile trend of
12 precipitation based on an interpolation of the 17 rain gauges that are within 25 km of the
13 catchment.

Formatted: English (New Zealand)

Formatted: English (New Zealand)

14 Denudation rates for the Rio Pisco have been measured by *Abbühl et al.* [2011] and
15 complemented by *Bekaddour et al.* [2014]. We use a tensioned spline (weight 0.1) to
16 interpolate denudation rate values for each point along the river profile. Denudation rates
17 reach a maximum of ~250 mm/ky in the knickzone and are much lower on both the plateau
18 and near the coast at ~11 mm/ky. We exclude one sample (Pis 11) from the dataset of *Abbühl*
19 *et al.* [2011] as it is most likely heavily influenced by recycling of shielded sand from the
20 ~50ky conglomerate terraces and therefore does not represent the basin-wide denudation rate
21 at this point. These long-profile values are used as inputs to calculate soil depths along the
22 Pisco Valley and to determine sediment delivery to the channel.

Formatted: English (New Zealand)

Formatted: English (New Zealand)

Formatted: English (New Zealand)

Formatted: English (New Zealand)

24 **4.2 Sediment load and transport**

25 Calculated modern sediment transport capacity and sediment flux (determined from ¹⁰Be
26 derived denudation rates (*Abbühl et al.* [2011]) show that the transition from supply limit to
27 transport limit coincides with the upstream appearance of terraces (Figure 7a and b). Note that
28 supply and transport limits refer in this case to excess transport capacity and sediment load,
29 respectively. We also acknowledge that the terrace sediments represent primarily the bedload
30 flux while the cosmogenic nuclide-derived sediment flux is total bedload. As such, our

Formatted: English (New Zealand)

Formatted: English (New Zealand)

1 | estimated sediment loads are likely a maximum. Even if with this caveat, the stream is supply
2 | limited in the upper bedrock-floored sections, and transport limited further down where cut-
3 | fill terraces are abundant, and the modern river flows over a wide floodplain made up of
4 | gravelly sediments. In the case that the Rio Pisco basin maintains steady-state (e.g. the
5 | response time of the weathering system is faster than the rate of climate change), the main
6 | response to a doubling of precipitation rates (using eq. 6 for water flux, and eq. 5 for the
7 | erosional flux) from modern is for the stream to aggrade over a relatively short ~20 km long
8 | section below the knickzone (Figure 7a). During drier climates, the sediment transport
9 | capacity in this zone exceeds the loads as denudation rates are low. According to this
10 | simulation of wet and dry steady-states, extensive cut-and-fill terraces should only be
11 | common in a narrow band near the knickzone (Figure 7a). Farther downstream, sediment flux
12 | exceeds sediment transport capacity both during wet and dry phases and the stream primarily
13 | aggrades.

14 | A transient stripping scenario is suggested by the results of *Steffen et al.* [2009]. According to
15 | Figure 3 in their paper, the transition towards a more humid climate resulted in an episodic
16 | phase of erosion, where regolith was rapidly stripped from hillslopes below the plateau over
17 | ~10-15 ky, supplying large volumes of sediment to the trunk stream. These phases of fluvial
18 | aggradation are followed by waves of incision travelling back up valley. This suggests that an
19 | episodic phase of rapid hillslope stripping occurs, resulting in a large sediment pulse to the
20 | rivers, followed by a rapid drop off of hillslope-derived sediment as the hillslope reservoirs
21 | are emptied. We model this transient response towards a more humid climate as a two-step
22 | process. Upon initiation of the wet period, all weathered regolith (calculated from the model)
23 | below the plateau is stripped from the hillslopes and supplied to the stream. In the second
24 | step, the bare hillslopes are unable to contribute new sediment to the stream. This is
25 | exacerbated by potentially faster erosion rates during the wet phases that inhibit the formation
26 | of a significant regolith cover. In this scenario, sediment supply to the stream during this step
27 | is controlled solely by inputs from the plateau, with little to no sediment being supplied from
28 | below the plateau. This pulsed-transient case necessitates that sufficient time has elapsed
29 | between wet periods for the weathered regolith to build up to the steady state values
30 | (*Bekaddour et al.*, 2014). This is the case for the $\sim 10^4$ yr climate intervals in western Peru
31 | (e.g. *Norton et al.*, 2014). The result of this simulation is that sediment accumulates over the
32 | entire downstream reach of the stream as regolith is rapidly stripped from the hillslopes. Once
33 | this material is exhausted, however, the bedrock-alluvial transition moves approximately 100

Formatted: English (New Zealand)

Formatted: English (New Zealand)

1 km upstream, incising the valley fill (Figure 7). This scenario is more consistent with the
2 observed occurrence of terraces in the Rio Pisco (Figure 3). This scenario is also supported by
3 ^{10}Be -derived paleodenudation rates (Figure 6; *Bekaddour et al.*, 2014). The first sediments
4 deposited during each wet phase are debris flow breccias with high ^{10}Be concentrations
5 (lower palaeodenudation rates), indicative of long residence time on the hillslopes. The
6 subsequent fluvial gravels are derived from sediment with shorter residence times (higher
7 palaeodenudation rates). The continued contribution of fluvial sediment with high
8 palaeodenudation rates suggests that reality most likely lies between the steady-state and
9 pulsed-transient cases. However, these end-member scenarios can be informative for
10 understanding terrace formation in escarpment environments

11

12 **5 Discussion and Conclusion**

13 Fluvial aggradation in the Rio Pisco has been associated with wet periods (*Steffan et al.*,
14 2009). This has important consequences for regolith production on the Western Escarpment.
15 On the plateau, where precipitation rates are ~1000 mm/yr and denudation rates ~10 mm/ky,
16 the response time of soils is > 100 ky (*Norton et al.*, 2014). In the knickzone, precipitation is
17 ~100-400 mm/yr and denudation rates are 100-250 mm/ky. This results in soil response times
18 of ~< 10ky. More importantly, the knickzone reach lies in a special climatic and denudational
19 setting in which small decreases in precipitation or increases in denudation can push the
20 system into a state where regolith production rates are unable to keep up with denudation.
21 Once conditions become amenable to regolith formation again, cover can reform on
22 millennial timescales on the hillslopes due to the rapid response times (*Norton et al.*, 2014).

23 When applied to the modern Rio Pisco the model suggests transient behavior. On the long
24 term, knickzone migration is eroding into the plateau as the river adjusts to a lower baselevel.
25 In addition to the direct control that baselevel has on the river, undercutting can dramatically
26 change the rates and style of hillslope response (Roering et al., 2015; Bilderbach et al., 2015).
27 In the Pisco Valley case, little sediment is available in the knickzones and response may
28 resemble the Waipaoa catchment in New Zealand where baselevel lowering generated
29 abundant deep-seated landslides (Bilderbach et al., 2015). Such a response is partially
30 supported by the presence of large boulders in the channels and coarse-angular clasts in the
31 debris flow deposits. On the short term, hillslopes are quickly stripped of sediment,
32 decoupling hillslope regolith from the incising channel. Key to both of these processes is that

Formatted: English (New Zealand)

1 the timescale of hillslope stripping (as implied by the occurrence of debris flows) is less than
2 the timescale of regolith production. For instance, an increase in precipitation rates can lead to
3 a temporary increase in denudation rates [Tucker and Slingerland, 1997] until the hillslopes
4 are stripped of sediment, exposing bedrock [Carson and Kirkby, 1972]. The regolith is then
5 regenerated during intermediate climates. An additional complication, recently suggested by
6 Heimsath et al. [2012], is that the maximum regolith production rate may also be dependent
7 on erosion rates such that faster erosion rates yield faster production rates. While we have not
8 built this relationship into this study; we note that such a relationship would lead to enhanced
9 regolith thickness in the knickzones and have no effect on the slowly eroding plateau or
10 coastal plains.

11 The model clearly shows that regolith production on hillslopes has a large impact on
12 sediment-flux in the river. The sequences of cut-fill terraces observed in the Rio Pisco are
13 more consistent with transient hillslope stripping during wet phases, followed by incision
14 once the hillslopes are bare of regolith. This can have significant consequences for the
15 evolution of bedrock streams in particular, where incision rates are at least partially dependent
16 on sediment flux [Whipple and Tucker, 2002]. It is interesting to note that much the terraced
17 zone does not adhere to the definition of a bedrock channel presented by Turowski et al.
18 (2008) since much of the erosion is acting on previous fill. In this case, the bedrock/alluvial
19 transition of Tucker and Slingerland (1996) is better defined as underload/overload with the
20 result being local erosion or deposition of the substrate, be it bedrock or sediment. Large
21 changes in sediment delivery will also result in significant changes in hydraulic geometry,
22 channel gradient, and erosion regime both at-a-station and downstream. Deposition during
23 high sediment load phases would flatten and widen the rivers, temporarily reducing driving
24 stress. For the transient case presented here, this would enhance the modelled relationship
25 leading to larger variation between erosional and depositional phases.

26 The occurrence of cut-fill terraces in the Rio Pisco is best explained by a pulsed-transient
27 response in which increased precipitation rates strip hillslopes of weathered material. The
28 hillslopes remain bare until climate again becomes amenable to the preservation of weathered
29 regolith. Such a scenario could be important in other escarpment settings.

31 Acknowledgements

Formatted: English (New Zealand)

Formatted: English (New Zealand)

Formatted: English (New Zealand)

Formatted: English (New Zealand)

Formatted: English (New Zealand)

Formatted: English (New Zealand)

Formatted: English (New Zealand)

1 | The authors would like to thank M. Trauerstein and T. Bekaddour for assistance in the field.

2 | This work was supported in part by a VUW Faculty of Science grant to KPN and SNE grant

3 | [200020_155892](#) awarded to FS.

4 |

Formatted: English (New Zealand)

Formatted: English (New Zealand)

Formatted: English (New Zealand)

References

Abbühl, L.M., Norton, K.P., Jansen, J., Schlunegger, F., Aldahan, A., and Possnert, G.: Landscape transience and mechanisms of ~~knickpoint~~ knickpoint retreat from ^{10}Be in the Western Escarpment of the Andes between Peru and northern Chile, *Earth Surface Processes and Landforms*, 36, 1464-1473, 2011.

Formatted: English (New Zealand)

Abbühl, L. M., Norton, K. P., Schlunegger, F., Kracht, O., Aldahan, A., and Possnert, G.: En Niño forcing on ^{10}Be -based surface denudation rates in the northwestern Peruvian Andes?, *Geomorphology*, 123, 257-268, 2010.

Agteca: Global Historical Climatology Network (GHCN-Monthly database) compilation for Peru, edited, Cochrane, T.A., Agteca.org, 2010.

Baker, P.A., Rigsby, C.A., Seltzer, G.O., Fritz, S.C., Lowenstein, T.K., Bacher, N.P., and Veliz, C.: Tropical climate changes at millennial and orbital timescales on the Bolivian Altiplano, *Nature*, 409, 698-701, 2001a.

Baker, P.A., Seltzer, G.O., Fritz, S.C., Dunbar, R.B., Grove, M.J., Tapia, P.M., Cross, S.L., Rowe, H.D., and Broda, J.P.: The History of South American Tropical Precipitation for the Past 25,000 Years, *Science*, 291, 640-643, 2001b.

[Bekaddour, T., Schlunegger, F., Vogel, H., Delunel, R., Norton, K.P., Akcar, N., and Kubik, P.K.: Paleo erosion rates and climate shifts recorded by Quaternary cut-and-fill sequences in the Pisco valley, central Peru, *Earth and Planetary Science Letters*, 390, 103-115, 2014.](#)

[Bilderback, E. L., Pettinga, J. R., Litchfield, N. J., Quigley, M., Marden, M., Roering, J. J., and Palmer, A.S.: Hillslope response to climate-modulated river incision in the Waipaoa catchment, East Coast North Island, New Zealand, *Geological Society of America Bulletin*, 127, 131-148, 2015.](#)

[Bloschl, G., Sivapalan, M., Wagener, T., Viglione, A., and Savenije, H.: Runoff Prediction in Ungauged Basins. Synthesis across Processes, Places and Scales Cambridge University press, 2013.](#)

Formatted: English (New Zealand)

Bookhagen, B., and Strecker, M.R.: Orographic barriers, high-resolution TRMM rainfall, and relief variations along the eastern Andes, *Geophysical Research Letters*, 35, 2008.

1 Bookhagen, B., D. Fleitmann, K. Nishiizumi, M. R. Strecker, and Thiede, R.C.: Holocene
2 monsoonal dynamics and fluvial terrace formation in the northwest Himalaya, India, *Geology*,
3 34, 601-604, 2006.

4 Carson, M. A., and Kirkby, M.J.: *Hillslope Form and Process*, Cambridge University Press,
5 Cambridge, 1972.

6 Fritz, S.C., Baker, P.A., Lowenstein, T.K., Seltzer, and Rigsby, C.A.: Hydrologic variation
7 during the last 170,000 years in the southern hemisphere tropics of South America,
8 *Quaternary Research*, 61, 95-104, 2004.

9 Hancock, G.S., and Anderson, R.S.: Numerical modeling of fluvial strath-terrace formation in
10 response to oscillating climate, *GSA Bulletin*, 114, 1131-1142, 2002.

11 Heller P.L., and Paola, C.: The large-scale dynamics of grain-size variation in alluvial basins
12 2: application to syntectonic conglomerate: *Basin Research*, 4, 91– 102, 1992.

13 [Heimsath, A.M., Dietrich, W.E., Nishiizumi, K., and Finkel, R.C.: The soil production
14 function and landscape equilibrium, *Nature*, 388, 358-361.](#)

15 [Heimsath, A.M., R.A. DiBiase, and Whipple, K.X.: Soil production limits and the transition
16 to bedrock-dominated landscapes, *Nature Geoscience*, 1-5, 2012.](#)

17 Kober, F., F. Schlunegger, G. Zeilinger, and Schneider, H.: Surface uplift and climate change:
18 the geomorphic evolution of the Western Escarpment of the Andes of northern Chile between
19 the Miocene and present, *Geological Society of America, Special Paper 398*, 97-120, 2006.

20 Leopold, L.B., M.G. Wolman, and Miller, J.P.: *Fluvial processes in geomorphology*, W.H.
21 Freeman and Company, San Francisco, 1964.

22 [LillyLitty, C., Duller, R., and Schlunegger, F.: Paleohydraulic reconstruction of a 40 kyr-old
23 terrace sequence implies that water discharge was larger than today, *Earth Surface Processes
24 and Landforms*, \[in review in press\]\(#\).](#)

25 Matmon, A., P. Bierman, and Enzel, Y.: Pattern and tempo of great escarpment erosion,
26 *Geology*, 30, 1135-1138, 2002.

27 McPhillips, D., Bierman, P.R., and Rood, D.H.: Millennial-scale record of landslides in the
28 Andes consistent with earthquake trigger, *Nature Geoscience*, 7, 925-930, 2014.

Formatted: English (New Zealand)

Formatted: English (New Zealand)

Formatted: English (New Zealand)

1 Meyer-Peter, E., and Müller, R.: Formulas for Bed-Load transport, Proceedings of the 3rd
2 Conference, International Association of Hydraulic Research, Stockholm, Sweden 39–64,
3 1948.

4 Norton, K.P., Molnar, P., and Schlunegger, F.: The role of climate-driven chemical
5 weathering on soil production, *Geomorphology*, 204, 510-517, 2014.

6 Placzek, C., Quade, J., and Patchett, P.J.: Geochronology and stratigraphy of late Pleistocene
7 lake cycles on the southern Bolivian Altiplano: Implications for causes of tropical climate
8 change, *Geological Society of America Bulletin*, 118, 515-532, 2006.

9 Roering, J. J., Mackey, B. H., Handwerger, A. L., Booth, A. M., Schmidt, D. A., Bennett, G.
10 L., and Cerovski-Darriau, C.: Beyond the angle of repose: A review and syn- thesis of
11 landslide processes in response to rapid uplift, Eel River, Northern California,
12 Geomorphology, 236, 109-131, 2015.

13 Schildgen, T. F., K. V. Hodges, K. X. Whipple, P. W. Reiners, and Pringle, M.S.: Uplift of
14 the western margin of the Andean plateau revealed from canyon incision history, southern
15 Peru, Geology, 35, 523-526, 2007.

16 Schlunegger, F., G. Zeilinger, A. Kounov, F. Kober, and Hüsser, B.: Scale of relief growth in
17 the forearc of the Andes of Northern Chile (Arica latitude, 18°S), *Terra Nova*, 18, 217-223,
18 2006.

19 Seidl, M. A., J. K. Weissel, and Pratson, L.F.: The kinematics and pattern of escarpment
20 retreat across the rifted continental margin of SE Australia, *Basin Research*, 8, 301-316, 1996.

21 Steffen, D., F. Schlunegger, and Preusser, F.: Drainage basin response to climate change in
22 the Pisco valley, Peru, *Geology*, 37, 491-494, 2009.

23 Tucker, G. E., and Slingerland, R.L.: Erosional dynamics, flexural isostasy, and long-lived
24 escarpments: a numerical modeling study, *Journal of Geophysical Research-Solid Earth and*
25 *Planets*, 99, 12,229-12,243, 1994.

26 Tucker, G. E., and Slingerland, R.L.: Drainage basin responses to climate change, *Water*
27 *Resources Research*, 33, 2031-2047, 1997.

28 Turowski, J.M., Hovius, N., Wilson, A., and Horng, M-J.: Hydraulic geometry, river sediment
29 and the definition of bedrock channels, Geomorphology, 99, 26-38, 2008.

Formatted: English (New Zealand)

1 [van der Beek, P., Summerfield, M. A., Braun, J., Brown, R. W., and Fleming, A.: Modeling](#)
2 [postbreakup landscape development and denudational history across the southeast African](#)
3 [\(Drakensberg Escarpment\) margin, Journal of Geophysical Research-Solid Earth, 107\(B12\),](#)
4 [2002.](#)

5 Vanacker, V., von Blanckenburg, F., Hewawasam, T., and Kubik, P.W.: Constraining
6 landscape development of the Sri Lankan escarpment with cosmogenic nuclides in river
7 sediment, Earth and Planetary Science Letters, 253, 402-414, 2007.

8 von Blanckenburg, F.: The control mechanisms of erosion and weathering at basin scale from
9 cosmogenic nuclides in river sediment, Earth And Planetary Science Letters, 242, 223-239,
10 2006.

11 von Blanckenburg, F., Hewawasam, T., and Kubik, P.W.: Cosmogenic nuclide evidence for
12 low weathering and denudation in the wet, tropical highlands of Sri Lanka, Journal of
13 Geophysical Research-Earth Surface, 109(F3), 2004.

14 Weissel, J. K., and Seidl, M.A.: Influence of rock strength properties on escarpment retreat
15 across passive continental margins, Geology, 25, 631-634, 1997.

16 Whipple, K. X., and Tucker, G.E.: Implications of sediment-flux-dependent river incision
17 models for landscape evolution, Journal of Geophysical Research, 107, 1-20, 2002.

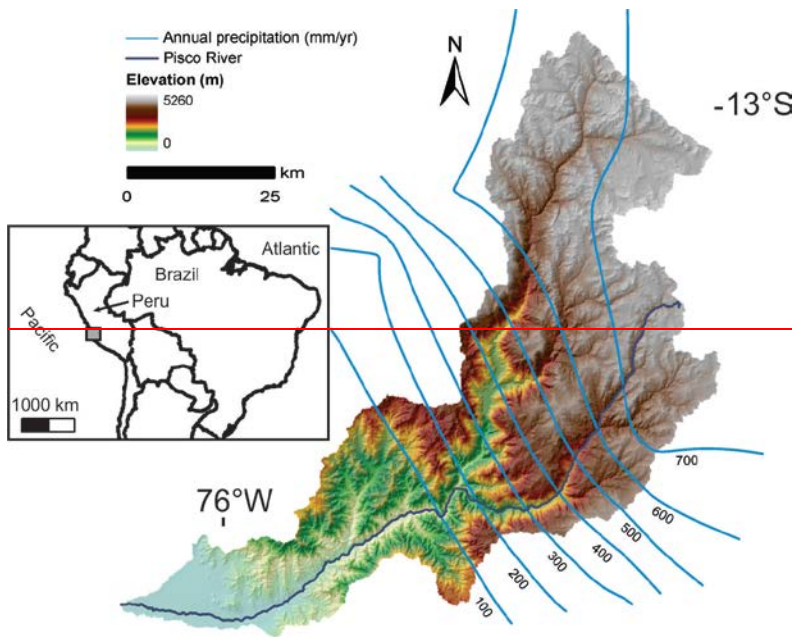
18 White, A. F., and Blum A.E.: Climatic effects on chemical weathering in watersheds;
19 application of mass balance approaches, in Solute modelling in catchment systems, edited by
20 S. T. Trudgill, 101-131, 1995a.

21 White, A. F., and Blum, A.E.: Effects of climate on chemical weathering in watersheds,
22 Geochimica et Cosmochimica Acta, 59, 1729-1747, 1995b.

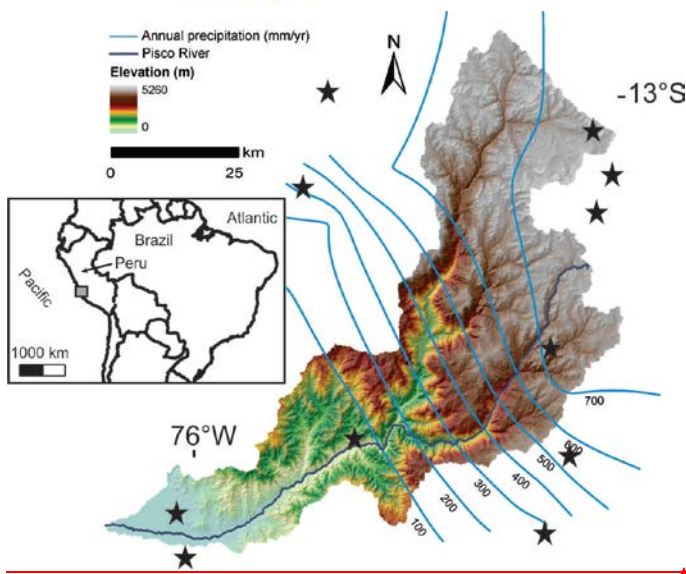
23 [Willet, S.D., McCoy, S.W., Perron, J.T., Goren, L., and Chen, C-Y.: Dynamic Reorganization](#)
24 [of River Basins, Science 343, 1249765-1-9.](#)

25 [Yalin, M. S.: River Mechanics, 219 pp., Pergamon, Tarrytown, N.Y., 1992.](#)
26

1



2



3

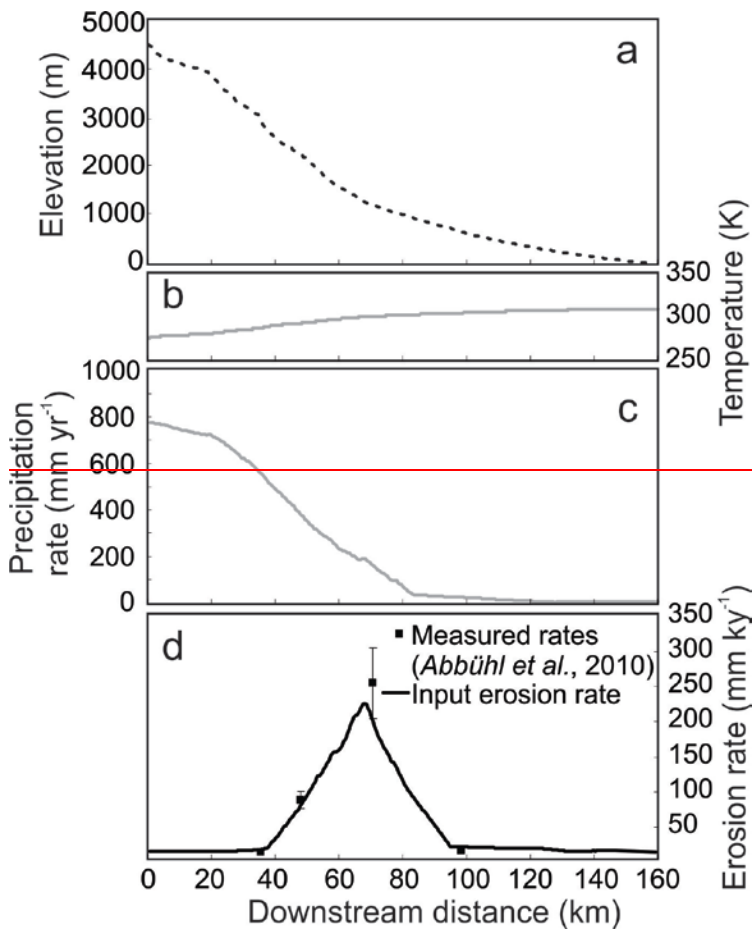
4

5

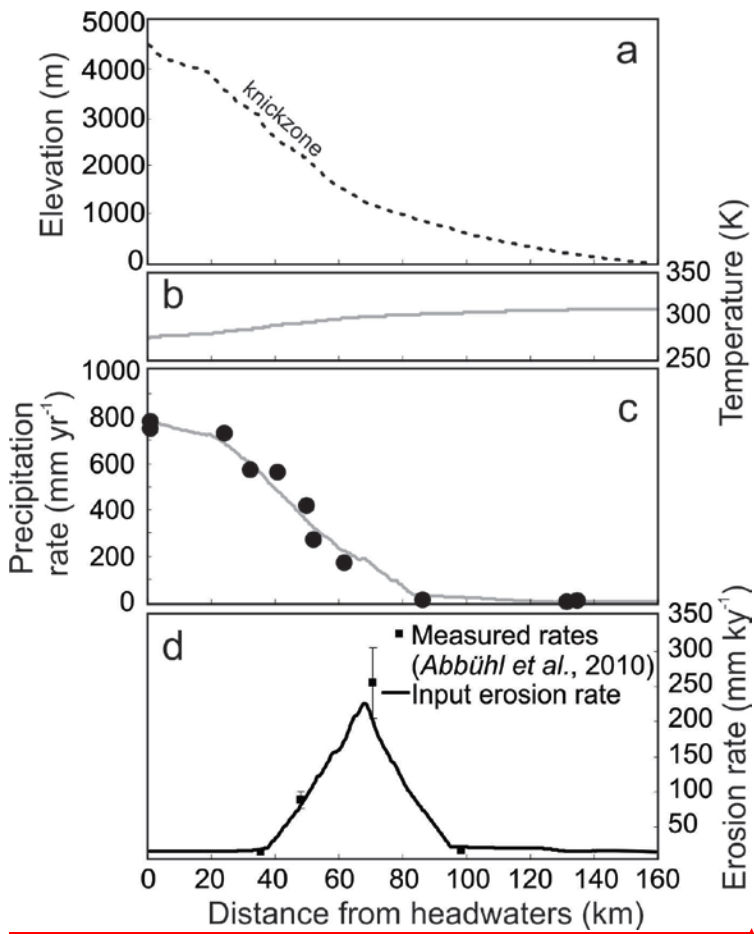
6

Figure 1. Setting and geomorphology of the Pisco River. Precipitation stations used to interpolate the annual rainfall are starred (Agteca, 2010).

Formatted: English (New Zealand)



1

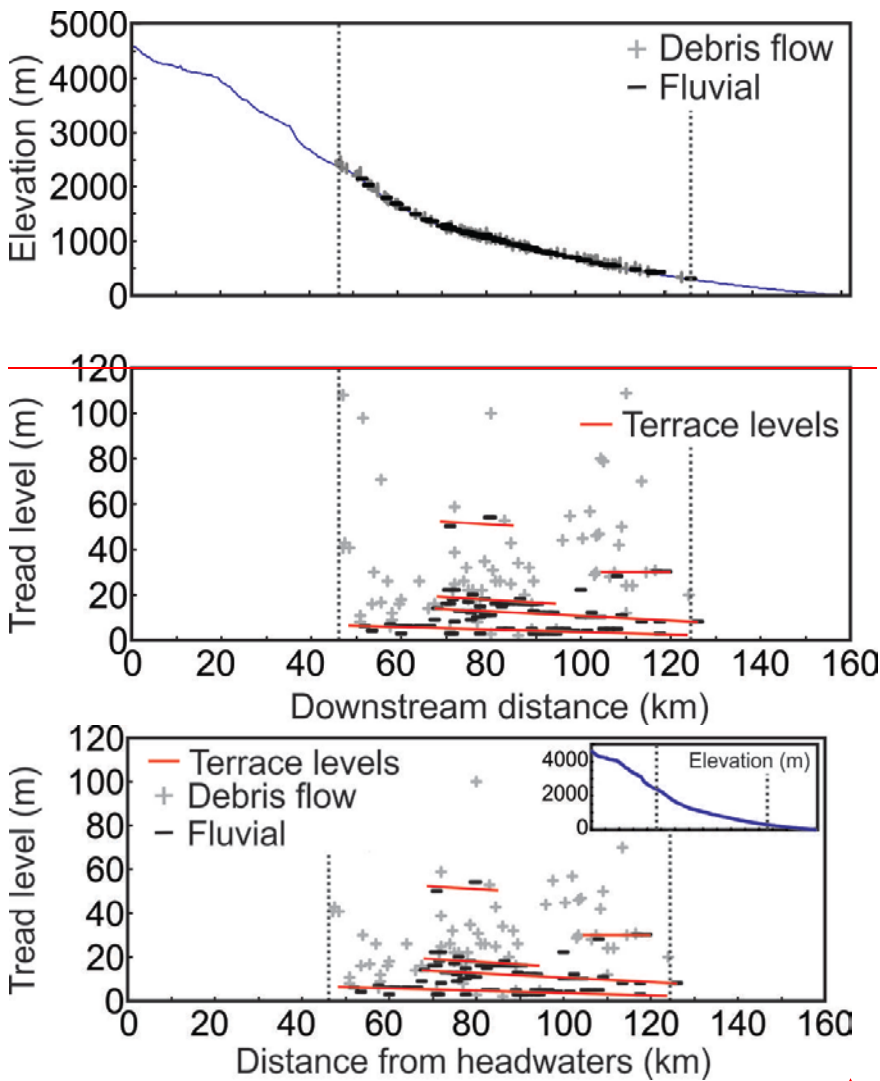


Formatted: English (New Zealand)

1
2
3
4
5
6
7
8

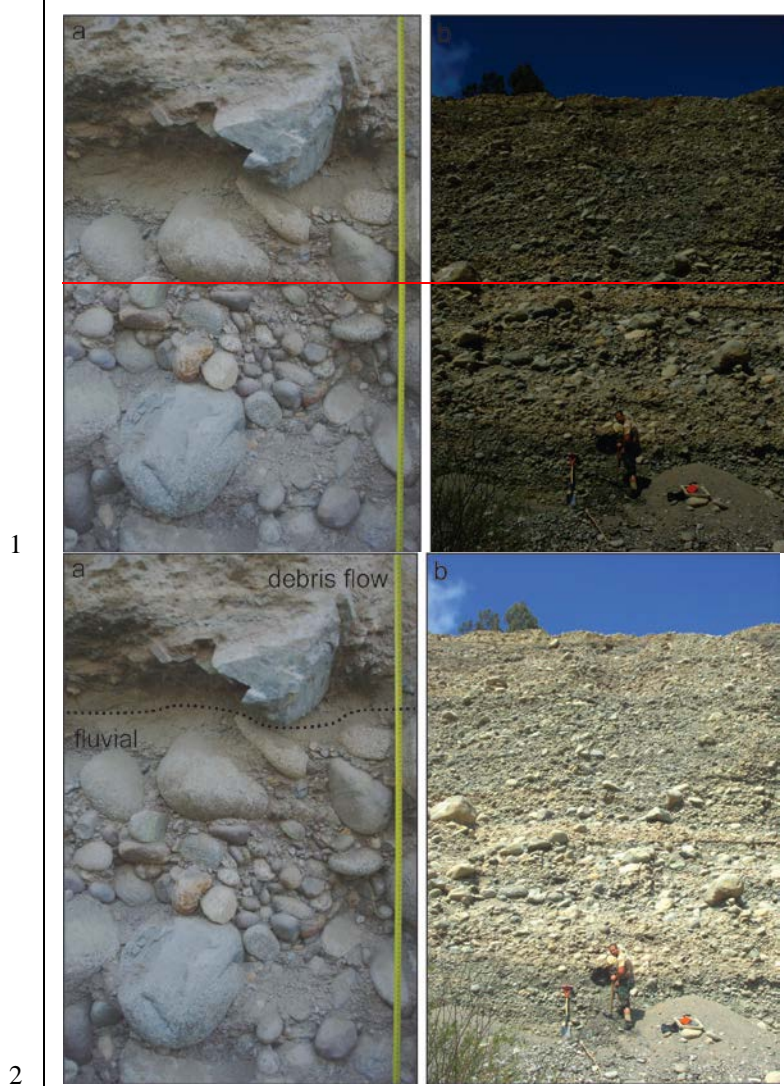
Figure 2. Geomorphic and climatic input parameters along the the Pisco River including: (a) river longitudinal profile, (b) temperature, (c) annual precipitation, and (d) erosion rate. Input rainfall stations (Agteca, 2010) projected along strike onto the Pisco River profile are shown by closed dots, input erosion rates with errors (Abbühl et al., 2010) are shown by closed squares.

Formatted: English (New Zealand)



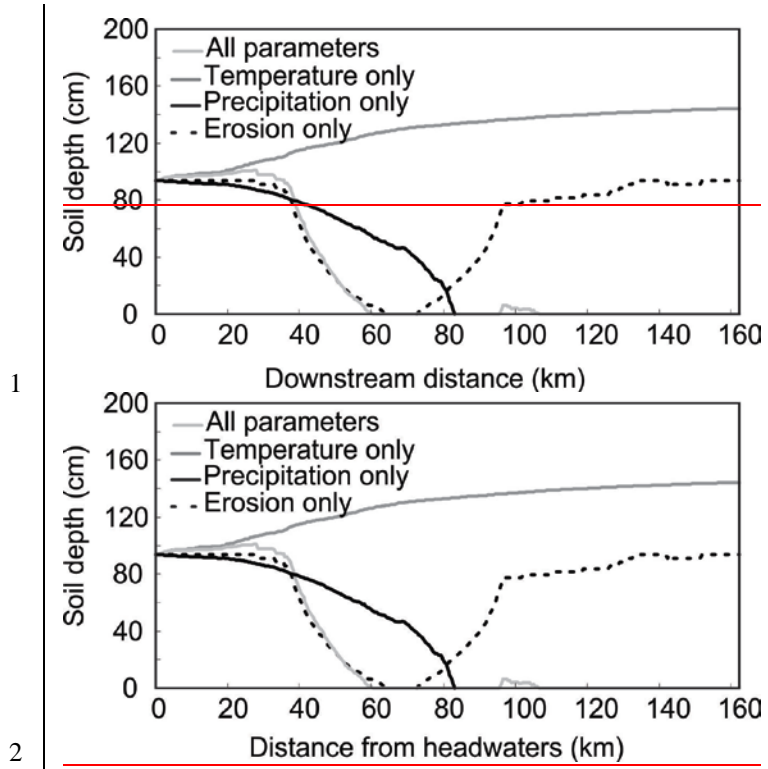
Formatted: English (New Zealand)

Figure 3. Locations of terraces along the Pisco River. The majority of terraces are concentrated in the zone from ~50 to 120 km downstream. Inset shows the location of the terraces (dashed lines) along the river profile.



4 Figure 4. Rapid soil stripping in the Pisco valley is evidenced by abundant debris flow
 5 deposits (top, a) mixed with coarse, poorly sorted fluvial deposits (bottom, a and b, note
 6 person for scale).

7



1

2

3

4 Figure 5. Sensitivity of the *Norton et al.* (2014) soil production model to each input parameter
 5 for the longitudinal profile of the Rio Pisco.

6

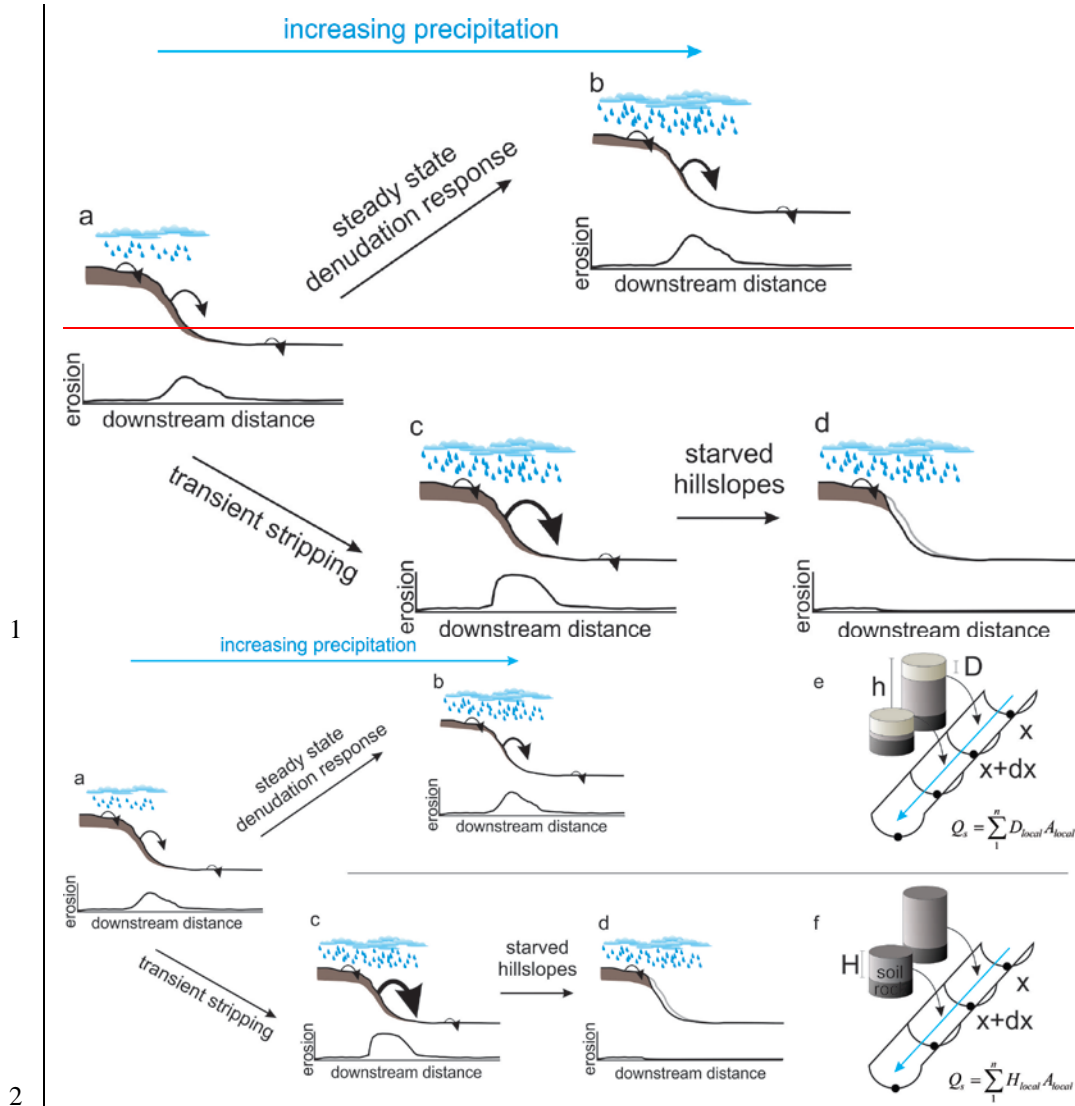
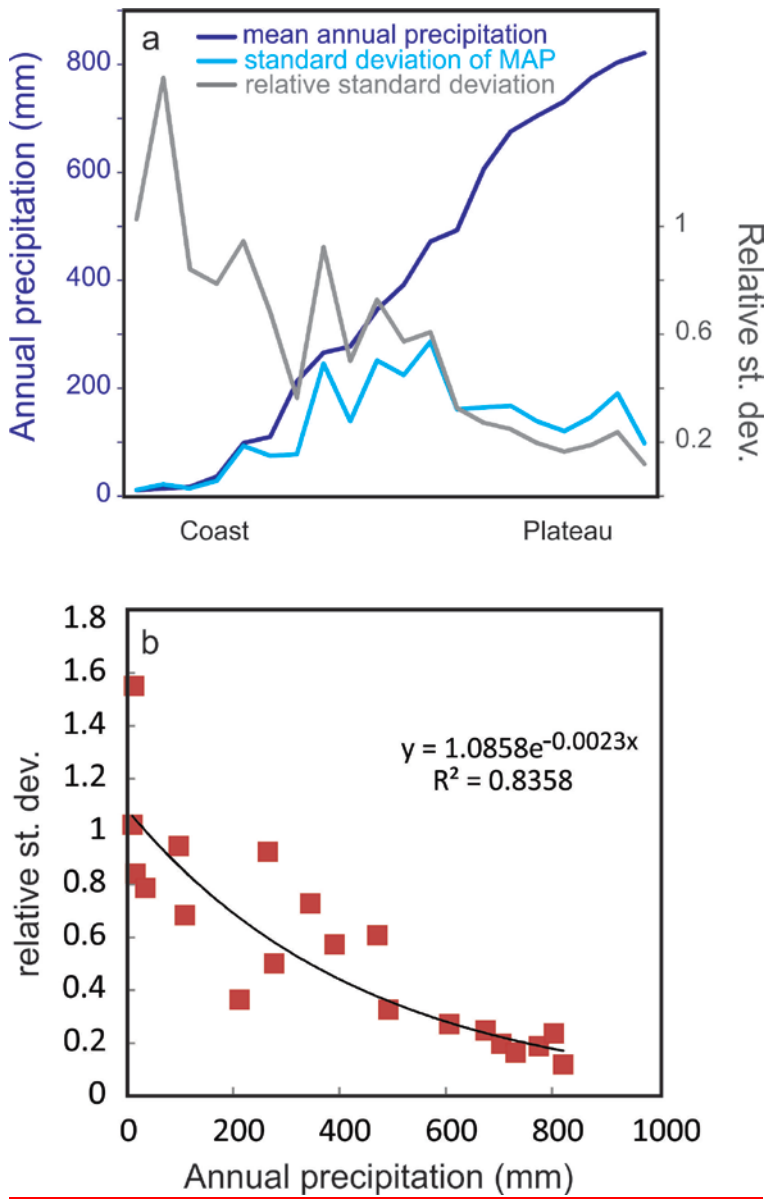
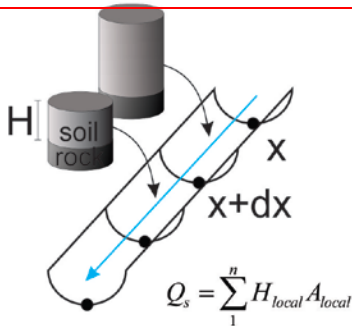
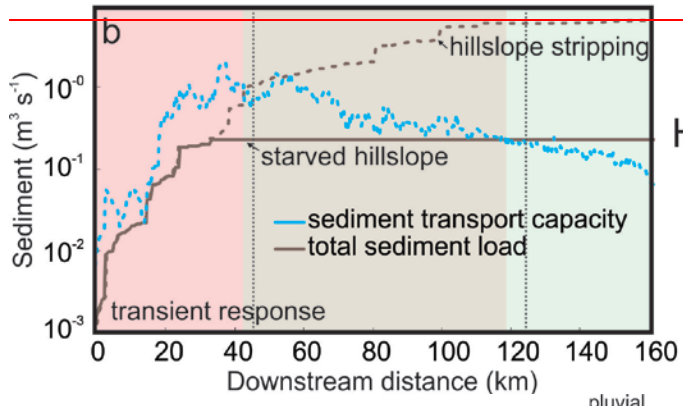
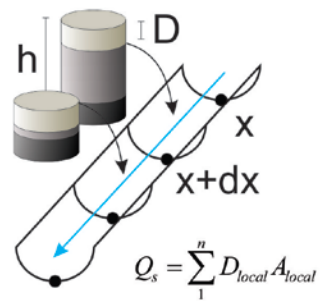
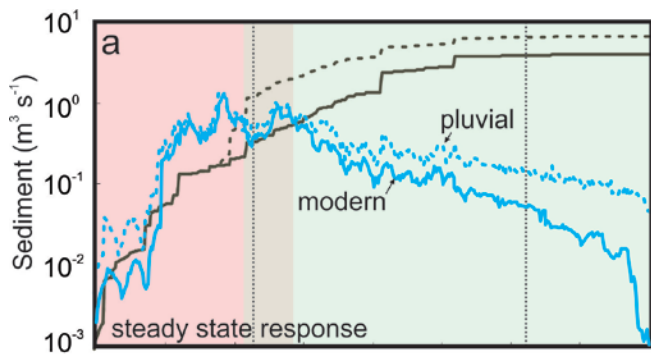


Figure 56. Conceptual model of two modes of hillslope response to increased precipitation in semi-arid environments. Arrow size represents the relative contribution of eroded hillslope sediment to the river. In the steady state case (a-b), increased precipitation results in increased hillslope erosion rates on steep hillslopes which are balanced by increased soil production (e.g. Norton *et al.*, 2014). In the transient case (a-c-d), increased precipitation results in rapid stripping of hillslope sediment as debris flows and shallow landslides (c), followed by

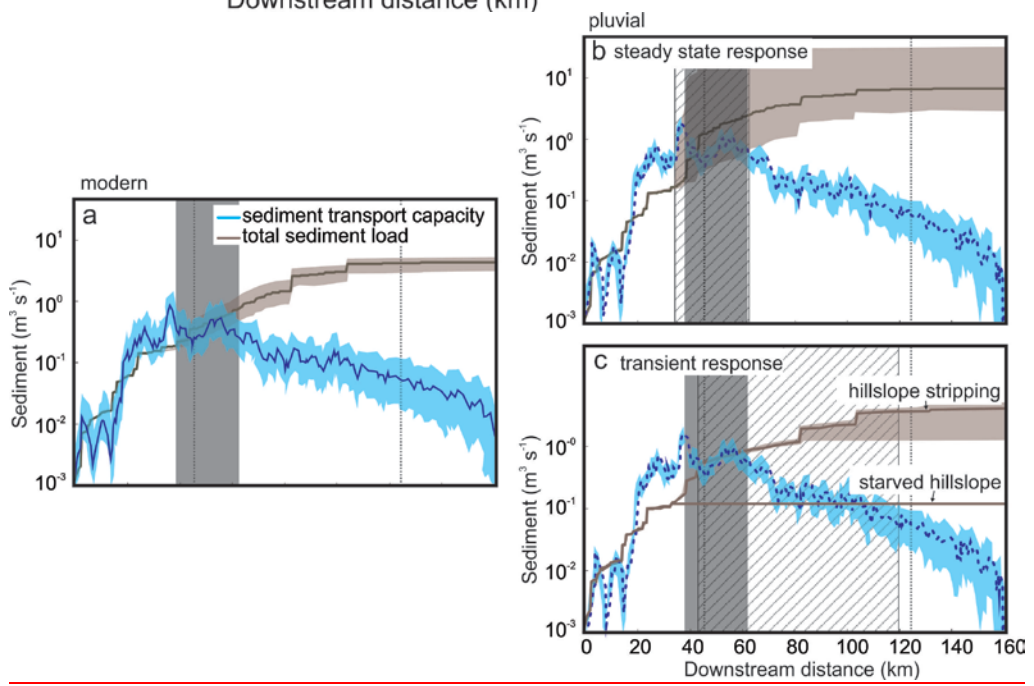
1 | negligible erosion on steep hillslopes once the soil mantle is eroded (d). The model set up for
2 | each of these scenarios is shown in e (steady state) and f (transient stripping).
3 |



1
 2 [Figure 7. Variation in annual precipitation calculated from monthly averages between 1960](#)
 3 [and 2003 \(Agteca, 2010\). The relative interannual variability is largest near the coast where El](#)
 4 [Nino years bring increased precipitation \(a\). The relationship between relative variability and](#)
 5 [annual precipitation \(b\) was applied to the soil production and transport models and carried](#)
 6 [through as uncertainty \(Figure 8\).](#)



1

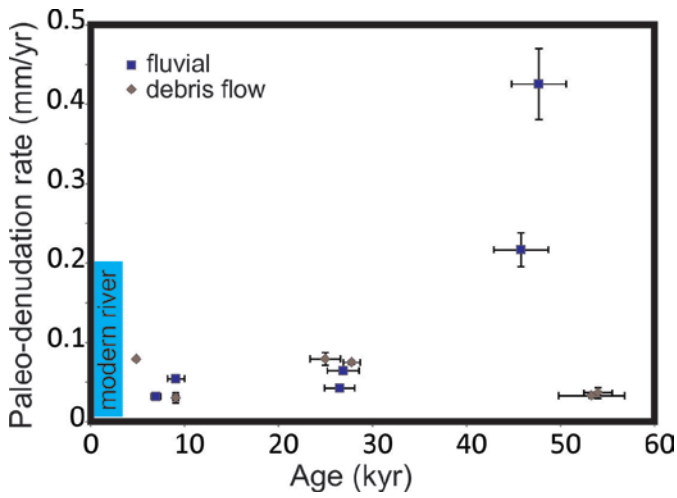


2

3

1 | Figure 78. Model of hillslope erosion through (a) steady state erosion and (b) transient
2 | hillslope stripping. In each graph, the solid grey area indicates the range of the modern
3 | bedrock/alluvial transition. The cross-hatched area indicates the endmember locations of the
4 | bedrock/alluvial transitions for each scenario. The grey stippled lines indicate the location of
5 | the Pisco River terraces. In the steady state case, the sediment load, Q_s , is proportional to the
6 | aerially summed upstream denudation rate, D , even if there is a thick regolith mantle, h . The
7 | result is a minimal shift in the bedrock/alluvial transition (the point at which sediment load
8 | exceeds sediment transport capacity; Tucker and Slingerland, 1997) between wet and dry
9 | phases (a). In the transient case, the entire modelled soil mantle (after Norton *et al.*, 2014) is
10 | stripped during a wet phase such that the sediment load, Q_s , is proportional to the aerially
11 | summed upstream regolith mantle, H , followed by a lack of sediment during the starved
12 | phase. The modelled result is a significant downstream shift in the bedrock/alluvial transition
13 | (b), which roughly corresponds to the observed occurrence of terraces in the Pisco valley.

14
15



1
2
3
4
5
6
7
8
9

Figure 8. Accelerated erosion following initial deposition of debris flow material supports the idea of rapid stripping of a stable regolith mantle. The initial high concentrations (low paleo-denudation rates) for the debris flow deposits could represent long residence time on hillslopes while the low concentrations (high paleo-denudation rates) for the fluvial material could be the result of rapid removal of the regolith cover (data after *Abbühl et al., 2011* and *Bekkadour et al., 2014*).

Formatted: English (New Zealand)